JOURNAL OF Materials CHEMISTRY

Two-component systems of isomorphous orientationally disordered crystals. Part 1 Packing of the mixed crystals

Josep Salud, David O. López, Maria Barrio and Josep Ll. Tamarit*

Departament de Física i Enginyeria Nuclear, Universitat Politècnica de Catalunya, E.T.S.E.I.B., Diagonal, 647 08028 Barcelona, Catalonia, Spain. E-mail: TAMARIT@FEN.UPC.ES

Received 26th October 1998, Accepted 27th January 1999

Five experimental two-component phase diagrams between orientationally disordered crystals (ODICs) have been established from the low-temperature phase to the liquid state using thermal analysis and X-ray powder diffraction techniques. The high-temperature orientationally disordered phases for the pure components, which belong to the series $(CH_3)_{4-n1}C(CH_2OH)_{n1}$ ($n_1=1,2,3$) and $(NO_2)(CH_3)_{3-n2}C(CH_2OH)_{n2}$ ($n_2=0,1$) are all face centered cubic. Continuous disordered mixed crystals in the whole range of concentration have been found, which indicates the existence of an isomorphism relationship. The intermolecular interactions in the ODIC state of these systems and other related two-component systems are discussed using the evolution of the packing coefficient as a function of the composition.

1 Introduction

Organic compounds characterised by globular or pseudo-globular molecules with weakly angle-dependent interactions are capable of forming orientationally disordered (ODIC)[1–4] phases (also called plastic phases) before the liquid state.

An extensive study has been undertaken for many years on the ODIC state from the investigation of single compounds in order to relate both macroscopic (heat capacity, phase transition, …) and microscopic (molecular dynamics, crystallographic structure, …) physical properties to the intermolecular interactions. These studies have been performed in most cases by analysing the dependence of some physical measurable properties as a function of one intensive variable, either temperature or pressure, in order to change the intermolecular interactions by modifying the local order in this kind of materials. A different way to modify these microscopic parameters consists of the change of the molecular surroundings by adding a guest molecule in the host crystal. Assuming that the geometry permits the substitution of a molecule of the host crystal and that the guest molecule does not possess the symmetry elements of the lattice, a symmetry simulation has been proved to be present.[5] Such a simulation is carried out by the guest molecule by achieving as many orientations as required by the symmetry of the crystallographic site of the host molecule. This well known rule[5] is of fundamental importance in the analysis of mixed crystals in the ODIC state, where a large number of possible energetically feasible orientations exist. Such experimental evidence has been found even in compounds whose molecules present some groups able to form strong interactions, either by means of hydrogen bonds or by the existence of large dipole–dipole interactions.[7–10] Many studies have concluded that the characteristic relaxation time of the overall tumbling in the ODIC state is considerably high when compared to similar molecules lacking these types of molecular interactions.[7] Moreover, the geometrical factor for orientationally disordered mixed crystals should play a decisive role. Nevertheless, it has been also well established for pure compounds that for an asymmetric molecule the reorientational motion has to couple with the lattice vibrations in order to make compatible its orientation in the ODIC state with the short-range repulsive forces of the neighbouring molecules in the generally close-packed lattice. This coupling between reorientational and vibrational modes produces a diminution of both the temperature range of the orientationally disordered phase and entropy change at the melting, because the vibrational modes must be activated during the reorientation itself.[11] This coupling is one of the most studied effects in organic materials displaying conventional glass phases.[12] A particular category is the so-called glassy crystal[13] which is obtained by freezing of the orientationally disordered phase of molecular crystals. Although the substitution of a guest molecule in the host crystal is not necessary to observe orientational freezing, several studies can be found where the disordered mixed crystals display the glassy state more readily.[13,14]

In the present study, which is part of the general framework of mixed crystals,[15–17] we have spanned a wider number of two-component systems[6,18,19] where the orientationally disordered phases of pure compounds are isostructural and thus are candidates to be isomorphous. In this first article we deal with the experimental systems as well as the establishment of common relations from a crystallographic point of view. In the following paper the thermodynamic mixing properties will be examined and a link between both points of view will be presented. To do so, several pure substances which are branched or tetrahedral molecules belonging to the series $(CH_3)_{4-n1}C(CH_2OH)_{n1}$ ($n_1=1,2,3$) and $(NO_2)(CH_3)_{3-n2}C(CH_2OH)_{n2}$ ($n_2=0,1$) have been considered. Whatever the substance, strong molecular interactions by means of hydrogen bonds or dipole–dipole intermolecular interactions ($n_2=0$) are displayed.

2 Experimental

2.1 Materials

The pure materials were purchased from Aldrich Chemical Company with a purity of 99%. They were submitted to an additional purification process consisting in a repeated vacuum sublimation at 313 K for $n_1=1$ [$(CH_3)_3C(CH_2OH)$, 2,2-dimethylpropan-1-ol, NPA], 343 K for $n_1=2$ [$(CH_3)_2C(CH_2OH)_2$, 2,2-dimethylpropane-1,3-diol, NPG], 393 K for $n_1=3$ [$(CH_3)C(CH_2OH)_3$, 1,1,1-tris(hydroxymethyl)propane, PG] and 353 K for $n_2=1$ ($(NO_2)(CH_3)_2C(CH_2OH)$, 2-methyl,2-nitropropan-1-ol, MNP). For $n_2=0$ [$(NO_2)C(CH_3)_3$, 2-methyl,2-nitropropane, TBN] the sublimation was performed under a low-pressure Ar atmosphere at 303 K. Molecular sieves were initially mixed with all the materials. Two-component mixtures were prepared from the melt of the pure materials in the selected composition by slow cooling (*ca.*

2 K min^{-1}) to room temperature. The samples invariably were treated under a controlled Ar atmosphere.

2.2 Thermal analysis

All the transition temperatures of the two-component systems as well as enthalpy changes were determined by means of a Perkin-Elmer DSC-7 calorimeter equipped with a home-made cooling attachment which enables temperatures of *ca.* 140 K to be attained in a control mode. The powder samples sealed into aluminium calorimetric cells weighed between 5 and 10 mg. Heating and cooling rates of 2 K min^{-1} were typically used. The solid–solid transition of CCl_4 and the melting of In were used for temperature and energy calibration.

The characteristic temperatures of the equilibria were determined from the thermograms using the shape factor method.[20]

C_p measurements for the glassy transitions were performed with a commercial modulated DSC TA2910 system from TA Instruments Inc. equipped with a cooling accessory which enables cooling to *ca.* 130 K. A heating rate of 2 K min^{-1}, a modulation amplitude of the sample temperature of ± 0.2 or ± 0.5 K and a period of 60 s were chosen over the temperature range. Sample masses were *ca.* 5–10 mg and, as previously, sapphire was used for calibration.

2.3 X-Ray powder diffraction

X-Ray powder diffraction measurements were performed with a horizontally mounted INEL cylindrical position-sensitive detector (CPS-120)[21] equipped with a liquid nitrogen INEL CRYO950 (80–330 K). The detector, placed in Debye–Scherrer geometry, permits a simultaneous recording of the powder pattern over the range of $2\theta = 0$–120°. Monochromatic Cu-Kα_1 radiation was selected with an asymmetric focusing incident beam curved quartz monochromator ($\lambda = 1.54059$ Å). The beam section was 6.3 mm high by 0.3 mm wide. The powdered samples were sealed into 0.5 mm Lindemann capillaries which rotate during the measurement in order to improve the averaging of the crystallites. External calibration using the cubic phase of $Na_2Ca_3Al_2F_4$ (NAC)[22,23] was applied in the range $2\theta = 0$–55° due to the lack of reflections for higher angles. In the case of diffraction at constant temperature, acquisition times of 30 min for the patterns and 10 min of stabilisation time were used, with a slewing speed of 1 K min^{-1}. After the indexing of the patterns lattice parameters were refined by means of the AFMAIL program.

3 Results

3.1 Polymorphism of the pure components

3.1.1 TBN [$(NO_2)C(CH_3)_3$]. Solid TBN is known to occur in three different crystalline forms. Phase III (the structure of which is unknown, hereafter denoted as [D]) transforms to an orthorhombic structure[24] ([O]) where the molecules perform uniaxial rotations (C'_3) around the C–NO_2 axis (librational phase).[25–27] The high-temperature solid phase I is an orientationally disordered phase where the molecules display overall rotation. In spite of the large molecular dipole, previous studies[28] revealed no specific correlations, giving rise to a high symmetry fcc lattice.[24] The thermodynamic properties characterising the phase transitions as well as the lattice parameters for the different solid phases are gathered in Table 1.

3.1.2 MNP [$(NO_2)(CH_3)_2C(CH_2OH)$]. The low-temperature ordered form of MNP ([M]) transforms to an orientationally disordered face centered cubic phase, which remains up to the melting point. Several NMR and IR spectroscopic studies have revealed the existence of intramolecular hydrogen bonds between the nitro and hydroxylic groups, producing the existence of an equilibrium between several conformers.[30,31] The thermodynamic and crystallographic parameters are given in Table 1.

3.1.3 NPA [$(CH_3)_3C(CH_2OH)$]. The low-temperature ordered phase of NPA ([T]) has been recently determined to be triclinic.[33] This phase II transforms to an orientationally disordered phase I.[40] The latter phase is stable up to the melting at 329.8 K. The thermodynamic parameters of the phase transitions determined in this work (see Table 1) match quite well with previously reported values.[34,41]

It should be pointed out that the phase behaviour of NPA will have a strong influence on the two-component systems (Section 3.2) and, therefore it deserves special mention. The thermal hysteresis in the transition I–II depends on the cooling conditions. When NPA in its orientationally disordered phase I is cooled fast enough to prevent the transition towards the ordered phase II, the disordered system is supercooled and a glassy state (I_g) is formed.[42] Such a state is characterised by the existence of the (average) translational order of the plastic phase with the orientational order partially frozen. It has been largely proved for this new condensed state that the averaged space groups of the plastic phase I, supercooled plastic phase I' and the glassy state (I_g) are all identical.[43,44] This property enables to the lattice parameter evolution with temperature to be readily monitored. Fig. 1 depicts the cubic lattice parameter for the I, I' and I_g phases as a function of temperature together with the volume expansivity. At 123 K a change in the expansivity, which is known to be a general thermodynamic signature of the glass transition,[45] is found. When increasing temperature from the glassy state, the relaxation phenomenon corresponding to the I_g–I' phase transition (at T_g) takes place. It should be pointed out that such a process is sample history dependent. At higher temperatures the supercooled phase I' can crystallise irreversibly to the stable phase II (this is the most common effect) or to a new intermediate metastable ordered phase (as for example in cyclohexanol[13]). As NPA behaves in the latter mode, single crystal studies would be needed in order to characterise the structural properties of this new metastable solid phase.

Owing to the low temperature value of the glass transition determined by X-ray powder diffraction, it was not possible to measure the heat capacity change associated with the relaxation effect by means of our calorimetric devices. In a previous reported work the dielectric relaxation time was studied in the plastic phase as a function of temperature and pressure.[41] It is well known that the glass transition occurs when the characteristic time of the isotropic reorientational motion reaches *ca.* 10^3 s,[46] whereas other possible anisotropic larger amplitude motions continue to exist within the glass state. The extrapolation of the relaxation time *vs.* temperature (at normal pressure) by considering an Arrhenius law corresponding to the above work[46] gives a temperature of *ca.* 125 K, which is certainly very close to the experimental temperature determined in this work. Nevertheless, in the neighbourhood of the glass transition non-Arrhenius behaviour might occur giving rise to significant differences between the extrapolated and the experimental values.

3.1.4 NPG [$(CH_3)_2C(CH_2OH)_2$]. The crystallographic properties of the low-temperature ordered ([M]) and ODIC phases[35,47,48] as well as the thermodynamic properties of the phase transitions[34] are given in Table 1. A recently published dielectric study on the disordered phase has revealed significant deviations from the single Debye relaxation, showing that strong intermolecular interactions *via* hydrogen bonds are present.[10] Such results confirm previous findings on the role played for those interactions which control the molecular packing in the mixed crystals of two-component systems.[18,19,49] On the other hand, a theoretical temperature (also calculated

Table 1 Summary of the crystallographic properties and the thermodynamic characteristics of the phase transitions for the pure components

		III–II			II–I			I–L	
	Formula	T/K	ΔH/kJ mol^{-1}	Phase II	T/K	ΔH/kJ mol^{-1}	Phase I	T/K	ΔH/kJ mol^{-1}
TBN	$(NO_2)C(CH_3)_3$	216.4[a]	4.34[a]	Orthorhombic[b] $a=10.280(6)$ Å $b=9.993(5)$ Å $c=6.205(4)$ Å $Z=4$, $T=233.2$ K	260.0[a]	4.64[a]	Fcc[b] $a=8.765(5)$ Å $Z=4$, $T=273.2$ K	298.5[a]	2.56[a]
MNP	$(NO_2)(CH_3)_2C(CH_2OH)$	—	—	Monoclinic $P2_1/c$[c] $a=6.195(3)$ Å $b=19.115(8)$ Å $c=16.601(9)$ Å $\beta=90.12(2)$ $Z=12$, $T=293.2$ K	311.5[a]	14.64[a]	Fcc[d] $a=8.857(10)$ Å $Z=4$, $T=356$ K	363.9[a]	3.17[a]
NPA	$(CH_3)_3C(CH_2OH)$	—	—	Triclinic[e] $a=10.304(10)$ Å $b=10.418(9)$ Å $c=11.398(12)$ Å $\alpha=90.14(6)^\circ$ $\beta=99.51(3)^\circ$ $\gamma=107.08(1)^\circ$ $Z=7$, $T=233.3$ K	235.4[a]	4.14[a]	Fcc[a] $a=8.815$ Å $Z=4$, $T=293$ K	329.8[a]	3.73[a]
NPG	$(CH_3)_2C(CH_2OH)_2$	60.4[f]	0.177[f]	Monoclinic $P2_1/n$[g] $a=5.979(1)$ Å $b=10.876(2)$ Å $c=10.099(2)$ Å $\beta=99.78(1)$ $Z=4$, $T=293.2$ K	314.4[a]	12.43[a]	Fcc[h] $a=8.854(8)$ Å $Z=4$, $T=353$ K	402.8[a]	4.34[a]
PG	$(CH_3)C(CH_2OH)_3$	—	—	Tetragonal $I\bar{4}$[i,j] $a=6.052(2)$ Å $b=8.872(3)$ Å $Z=2$, $T=293.2$ K	356.7[a]	20.94[a]	Fcc[k] $a=8.876(8)$ Å $Z=4$, $T=363$ K	474.4[a]	4.72[a]

[a]This work. [b]Ref. 24. [c]Ref. 29. [d]Ref. 32. [e]Ref. 33. [f]Ref. 34. [g]Ref. 35. [h]Ref. 36. [i]Ref. 37. [j]Ref. 38. [k]Ref. 39.

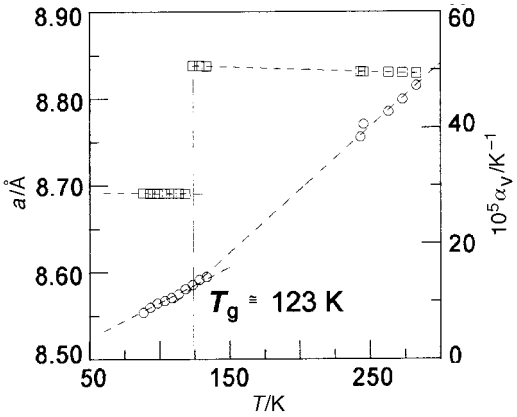

Fig. 1 Cubic lattice parameter (○) and volume expansivity (□) for plastic (I), supercooled (I′) and glassy state (I_g) phases *vs.* temperature for NPA $[(CH_3)_3C(CH_2OH)]$.

from the extrapolation of the relaxation time assuming an Arrehnius behaviour) corresponding to the freezing of the large-amplitude motions (glass transition) was determined to be *ca.* 120 K.

3.1.5 PG $[(CH_3)C(CH_2OH)_3]$. Basic crystallographic and thermodynamic data corresponding to the ordered and disordered phases and the phase transitions are listed in Table 1. Structural details can be found in references 6, 37 and 38.

3.2 Two-component systems

3.2.1 TBN–NPA system. The main characteristics of the TBN–NPA two-component (Fig. 2) system are the existence of a low-temperature peritectoid invariant (between *ca.* 0.03 and 0.94) concerning the [D + T + O] three-phase equilibrium at 217.9 K, a eutectoid invariant relating the three-phase equilibrium [O + T + C_F] at 227.8 K and a very narrow orientationally disordered–liquid loop. The eutectoid limiting points were determined to be at 0.02 and 0.94 by means of the Tammann diagrams.[50] Fig. 3 shows the enthalpy change for the orientationally disordered–liquid equilibrium as a function of the mole fraction.

Crystallographic study at 293.2 K. The continuous evolution of the lattice parameter *vs.* concentration for the fcc phase ($[C_F]$) at 293.2 K, shown in Fig. 4, together with the continuous evolution of the temperatures characterising the plastic–liquid equilibrium, prove the formation of orientationally disordered substitutional mixed crystals in the whole concentration range. In addition, this crystallographic characterisation shows that the orientationally disordered phase of TBN is isomorphous to that of the NPA, confirming the fcc lattice symmetry found recently for TBN[6] in contrast to previous works.[51]

3.2.2 TBN–MNP system. The experimental two-component phase diagram TBN–MNP from 223 K to the liquid state is shown in Fig. 2. The low temperature side of the phase diagram shows a eutectic invariant at 250.0 K in the range $x=0$–0.95 molar fraction of MNP (the eutectic point at $x\approx0.13$). Such values were obtained from the Tammann diagram associated to the eutectic transformation.[50] The influence of the phase transition III–II of TBN on this two-component system was not studied. The enthalpy change for the melting process as a function of the mole fraction is depicted in Fig. 3.

Crystallographic study at 293.2 K. In order to verify the possible isomorphic relationship between the disordered phases of the two components, an isothermal X-ray powder diffraction study in the molecular alloys was undertaken at 293.2 K. Moreover, this study enables analysis of the evolution of the volume of the unit cell as a function of the mole fraction at constant temperature. For samples with mole fraction $x\geqslant0.7$

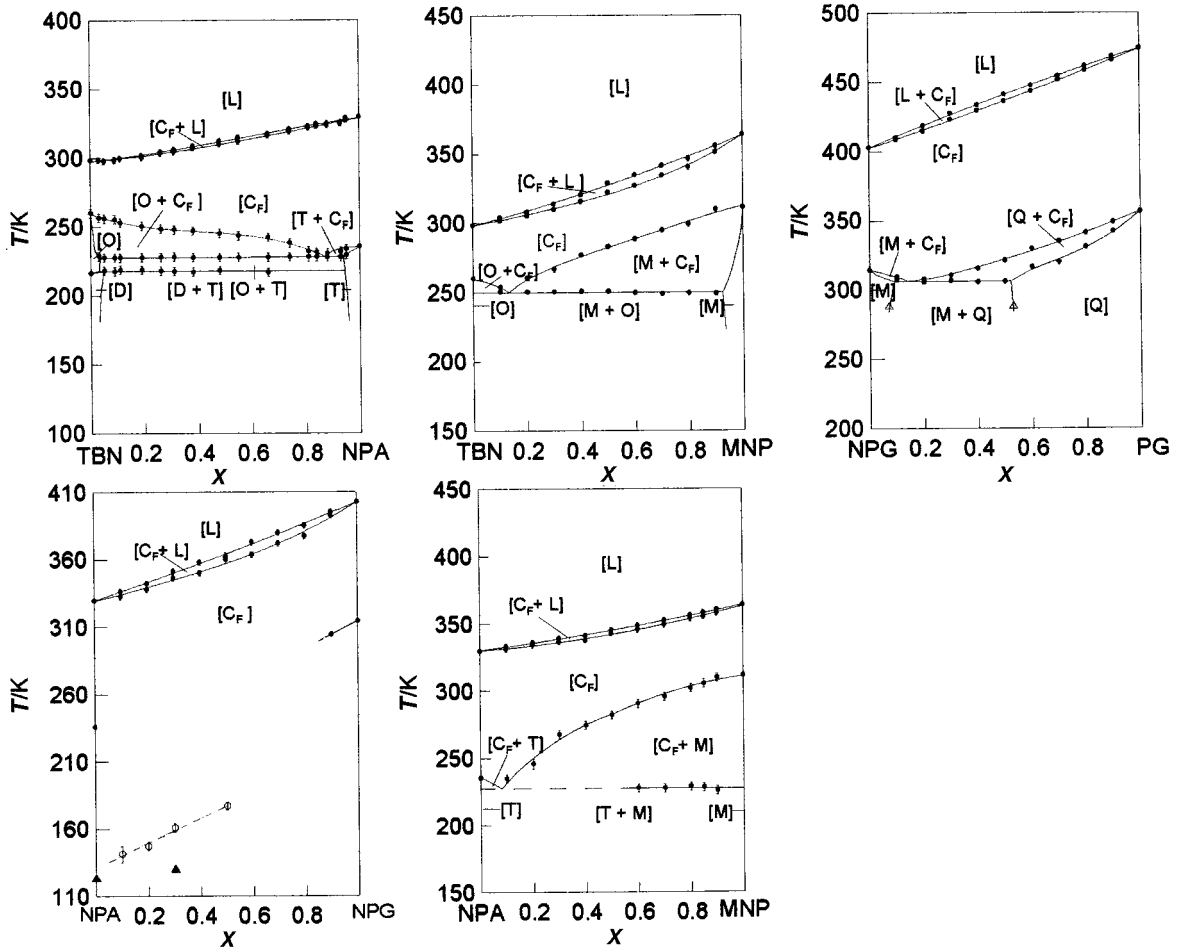

Fig. 2 Two-component phase diagrams. (●) Transition temperatures obtained from DSC measurements. The non-equilibrium glass transition temperatures (○) from C_p and (Δ) from X-ray powder diffraction measurements have been included in the equilibrium phase diagram for brevity. [L] Liquid phase; [M] monoclinic, [T] triclinic and [Q] tetragonal low-temperature ordered solid forms; [C_F] orientationally disordered fcc phase. (For compound abbreviations see Table 1.)

of MNP the two phases [M] and [C_F] coexist at 293.2 K. Therefore, the measurements for these samples were carried out on the experimentally metastable orientationally disordered phase. For the pure component MNP ($x=1$) it was not possible to retain its ODIC phase at 293.2 K, the lattice parameter at such temperature being obtained by means of its evolution with temperature between 323 and 303 K. Fig. 4 depicts the results corresponding to the continuous evolution of the lattice parameter with mole fraction.

3.2.3 NPG–PG system. The NPG–PG two-component system was published some time ago[32] and is now restudied due to the considerable difference in the melting temperatures of the pure components as a consequence of the purification process. The low-temperature side (Fig. 2) displays no qualitative changes with the previously published results. A small shift in the eutectoid temperature (at 306.5 K) as well as in the eutectoid composition is however seen. By contrast, the orientationally disordered–liquid equilibrium is determined to be a narrow loop, in contrast to the Gibbs minimum reported in ref. 52. The evolution of the enthalpy change for the melting of molecular alloys is depicted in Fig. 3. Some measurements by X-ray powder diffraction have been performed in order to determine the cubic lattice parameters for the molecular alloys at 356 K with no noticeable differences being found in relation to the previously published data.

3.2.4 NPA–NPG system. As in the previous two-component systems, NPA and NPG are found to be isomorphous in the ODIC state. As shown in Fig. 2, disordered mixed crystals melt in such a way that the two-phase orientationally disordered–liquid equilibrium is a loop. The enthalpy change of the molecular alloys in such a process is shown in Fig. 3.

Crystallographic study at 313.2 K. The variation of the cubic parameter as a function of mole fraction at 313.2 K is displayed in Fig. 4. The continuous evolution of this parameter *vs.* mole fraction together with the loop for the melting process enables us to establish the existence of continuous mixed crystals, *i.e.*, the establishment of an isomorphic relationship between the high-temperature disordered phases of both pure components NPA and NPG.

Glassy mixed crystals. Concerning the low-temperature phase equilibria between the orientationally disordered phase and the ordered triclinic (NPA) and monoclinic (NPG) phases, the DSC curves did not show the typical thermograms corresponding to the standard solid–solid transformations. In order to distinguish between the two possibilities, that is to say, metastable supercooled ODIC molecular alloys or the existence of a glassy state, C_p measurements at low temperature (from 130 K) as well as X-ray powder diffraction measurements (from 80 K) were performed. Results for the former are shown in Fig. 5 for several molecular alloys ($x \leqslant 0.5$) as a function of temperature. A typical relaxation process from the glassy state to the supercooled plastic phase characterised by a C_p change was found. The latter, performed on the $NPA_{0.7}NPG_{0.3}$ mixed crystal is shown in Fig. 6. The evolution of the cubic lattice parameter *vs.* temperature as well as the discontinuity on the lattice expansivity are the irrefutable signatures of the existence

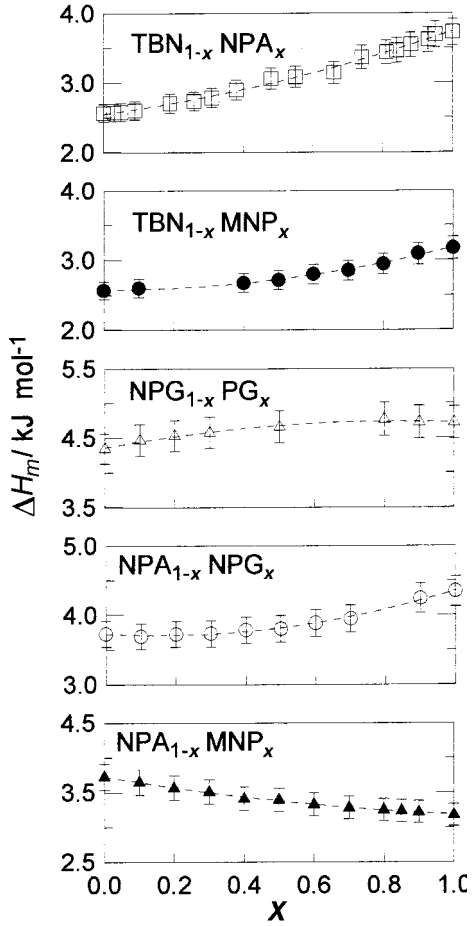

Fig. 3 Enthalpies of melting as a function of the composition for the orientationally disordered mixed crystals in the two-component systems. (For compound abbreviations see Table 1.)

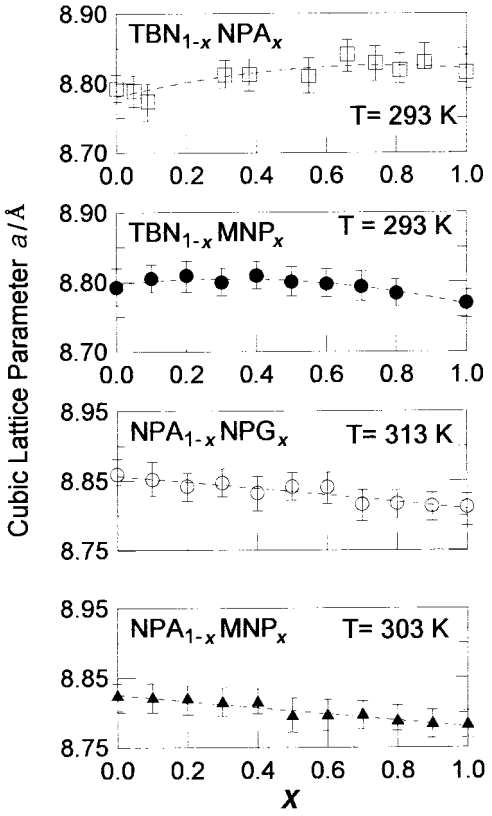

Fig. 4 Lattice parameter as a function of the composition for the cubic orientationally disordered mixed crystals for the two-component systems. (For compound abbreviations see Table 1.)

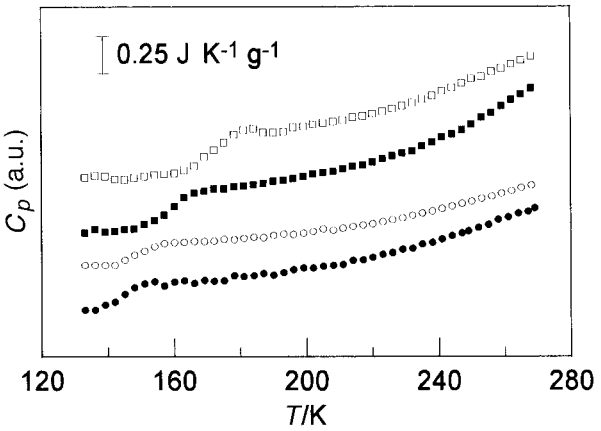

Fig. 5 C_p variation as a function of temperature for several $NPA_{1-x}NPG_x$ $\{[(CH_3)_3C(CH_2OH)]_{1-x}/[(CH_3)_2C(CH_2OH)_2]_x\}$ mixed crystals in the temperature range corresponding to the glass transition. (● $x=0.1$, ○ $x=0.2$, ■ $x=0.3$ and □ $x=0.5$.)

of a glassy state. Although the T_g temperature is not an equilibrium temperature, these values, as a function of the mole fraction, have been also included in the equilibrium phase diagram. Owing to the different time-scaling of the experimental techniques used, the T_g temperatures are relatively different. This fact explains the breakdown of the evolution of T_g *vs.* mole fraction shown in Fig. 2 between the pure component NPA and the mixed crystals. Unlike the preceding published examples concerning the formation of a glassy state in mixed crystals, such as those formed by chloroadamantane and cyanoadamantane,[14,44,52,53] a strong variation of T_g with the mole fraction is found. This fact shows that the freezing mechanisms are scarcely influenced in the presence of the guest molecule. It is also worth noting that this binary system displays a very interesting phase stability sequence which gives rise to a unique opportunity to study the dynamics of the glassy state as well as the supercooled plastic phase. On the one hand, the quench, which is necessary to by-pass the first-order phase transition toward the lower symmetry crystalline (ordered) phase to reach the glassy state, is easily achievable in these molecular alloys (cooling rates of *ca.* 2 K min^{-1} are required). On the other hand, after the glassy to supercooled ODIC phase transition has been carried out, the orientationally disordered phase is in a metastable situation with regard to the low-temperature ordered crystalline phase that remains until the temperature where it becomes stable. Therefore, the temperature domain where the dynamical behaviour of such phases can be studied is considerable and enables analysis of the evolution of physical properties *vs.* temperature.

For molecular alloys with mole fraction >0.5 the kinetic behaviour is different and the glassy state for any of the samples is not reached. Particularly, for the mixed crystals with $x \geqslant 0.9$ the ordered solid phase [M] is partially achievable giving rise to the possibility to obtain, in some cases, the upper solvus corresponding to the crystalline ordered (monoclinic)–orientationally disordered equilibrium. There was no mole fraction for which the necessary three-phase invariant $[T+M+C_F]$ was detected.

3.2.5 NPA–MNP system. The loop corresponding to the orientationally disordered–liquid equilibrium is depicted in Fig. 2. The associated enthalpy change for this melting process is shown in Fig. 3. With regard to the low temperature equilibria, the phase behaviour is strongly dependent on the mole fraction. For mole fractions $x \geqslant 0.6$ the DSC scans display signals corresponding to a three-phase eutectic equilibrium at

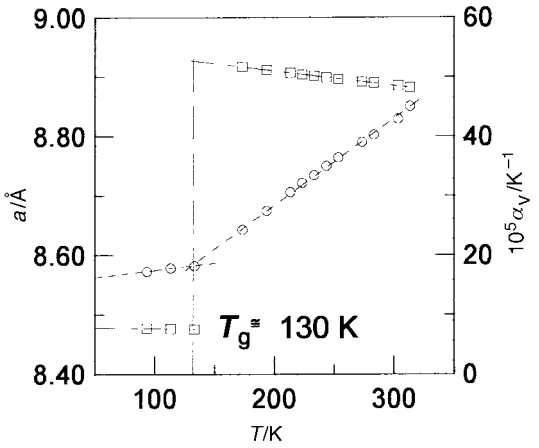

Fig. 6 Cubic lattice parameter (○) and volume expansivity (□) for plastic (I), supercooled (I′) and glassy state (I_g) phases *vs.* temperature for the $NPA_{0.7}NPG_{0.3}$ $\{[(CH_3)_3C(CH_2OH)]_{0.7}/[(CH_3)_2C(CH_2OH)_2]_{0.3}\}$ molecular alloy.

227.4 K, in addition to the upper solvus corresponding to the $[M+C_F]$ to $[C_F]$ transition. For mole fractions with $x \leqslant 0.5$ the thermodynamic equilibrium is not reached owing to the fact that the triclinic structure of the necessary limiting solid solution does not appear on cooling. Therefore, on the heating runs, only the upper solvus corresponding to the $[M+C_F]$ to $[C_F]$ transition is present. Such an experimental fact can be probably associated to the readiness of the orientationally disordered phases of NPA to be undercooled and subsequently to be frozen in a glassy state.[54] Unlike the previous two-component NPA–NPG system, no glass transition was detected for the low mole fraction samples in the experimentally available temperature domain.

Crystallographic study at 303.2 K. The continuous variation of the cubic lattice parameters of the disordered mixed crystals *vs.* mole fraction at 303.2 K (see Fig. 4) implies isomorphism between the orientationally disordered phases of NPA and MNP.

3.3 Packing of the orientationally disordered molecular alloys

Most of the ordered low-temperature structures of the compounds belonging to the series studied in this work $(CH_3)_{4-n1}C(CH_2OH)_{n1}$ and $(NO_2)(CH_3)_{3-n2}C(CH_2OH)_{n2}$ as well as similar series such as $(NH_2)(CH_3)_{3-n3}C(CH_2OH)_{n3}$ have been solved. The common feature is the existence of strong intermolecular interactions by means of the bonds generated by the –OH groups and, when present, $–NH_2$ groups. Nevertheless, owing to the disordered character of the high-temperature phase, no structures describing this form have been published for the mentioned compounds. In order to obtain information on the degree of interactions in molecular alloys, the approach proposed by Kitaigorodsky,[55] which relies on the analysis of the packing coefficient, has been used. Previous work has shown that this parameter is a powerful tool to account for intermolecular interactions in molecular alloys.[19,49]

The packing coefficient is defined as the ratio between the volume of the molecule V_m (or the average molecule for the molecular alloys) and the available volume in the lattice ($V_Z = V/Z$, where V is the unit-cell volume and Z is the number of molecules in the unit cell). The average molecular volume $V_m(x)$ for a given molecular alloy of mole fraction x can be assumed to be:

$$V_m(X) = (1-x)V_{mA} + xV_{mB}$$

where V_{mA} and V_{mB} are the molecular volume for the A and B components of the mixed crystal, respectively. Thus, the temperature- and composition-dependent packing coefficient $\xi(x,T)$ is defined as:

$$\xi(x,T) = \frac{(1-x)V_{mA} + xV_{mB}}{V_z(x,T)}$$

where $V_Z(x,T)$ is the available unit-cell volume per molecule of the molecular alloy.

In order to account for the influence of the substitution process in the molecular alloys by analysing the packing evolution *vs.* composition, the temperature effect must be avoided by measuring the lattice volume at constant T (as has been shown in previous sections). To evaluate V_m the molecules have been built up by means of the standard distances between atoms (irrespective of the type of molecule) and van der Waals radii. The values were taken from references 56–58. Table 2 summarises the calculated molecular volumes.

Fig. 7 depicts the evolution of the packing coefficient *vs.* composition for the preceding two-component systems analysed in the previous sections together with those formerly published. The B component of the $A_{1-x}B_x$ molecular alloy has been chosen as the molecule having the largest number of CH_2OH groups. Whatever the two-component system analysed, the experimental results confirm that the packing parameter is an increasing function of the number of potential intermolecular interactions by hydrogen bonds. To reinforce this idea, two additional experimental findings should be pointed out. On the one hand, the highest change in the packing coefficient on going from $x=0$ to 1 is determined

Table 2 Molecular volumes (V_m) for the pure components and ε_K values for the two-component systems

System A–B	V_{mA}/Å^3	V_{mB}/Å^3	ε_K
NPA–MNP $[(CH_3)_3C(CH_2OH)]$–$[NO_2(CH_3)_2C(CH_2OH)]$	102.6	103.7	0.904
NPA–NPG $[(CH_3)_3C(CH_2OH)]$–$[(CH_3)_2C(CH_2OH)_2]$	102.6	108.9	0.938
NPG–PG $[(CH_3)_2C(CH_2OH)_2]$–$[(CH_3)C(CH_2OH)_3]$	108.9	115.2	0.941
TBN–NPA $[NO_2C(CH_3)_3]$–$[(CH_3)_3C(CH_2OH)]$	97.4	102.6	0.882
TBN–MNP $[NO_2C(CH_3)_3]$–$[NO_2C(CH_3)_2(CH_2OH)]$	97.4	103.7	0.935
PG–PE $[(CH_3)C(CH_2OH)_3]$–$[C(CH_2OH)_4]$	115.2	121.4	0.946
MNP–NPG $[NO_2C(CH_3)_2(CH_2OH)]$–$[(CH_3)_2C(CH_2OH)_2]$	103.7	108.9	0.889
MNP–PG $[NO_2C(CH_3)_2(CH_2OH)]$–$[(CH_3)C(CH_2OH)_3]$	103.7	115.2	0.826
AMP–TRIS $[NH_2C(CH_3)(CH_2OH)_2]$–$[NH_2C(CH_2OH)_3]$	103.6	109.9	0.939

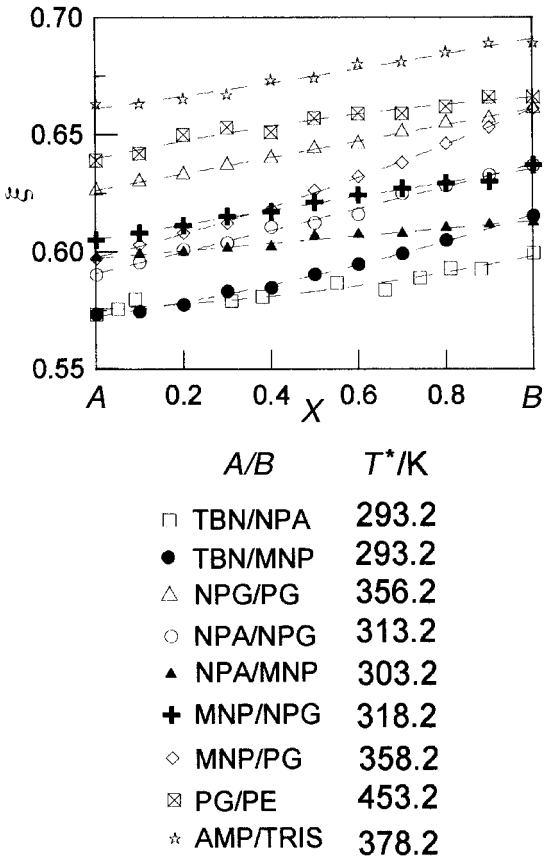

Fig. 7 Packing coefficient (ξ) at T^* as a function of composition of the cubic orientationally disordered mixed crystals for the two-component systems. (For compound abbreviations see Table 2.)

to be for the $MNP_{1-x}PG_x$ [$(NO_2)(CH_3)C(CH_2OH)$–$(CH_3)C(CH_2OH)_3$] molecular alloys, which corresponds to the system where the largest differences in the number of –CH_2OH groups exists, producing the largest differences in the intermolecular interactions for the pure components. On the other hand, the variation of the packing coefficient with the molar fraction for the system NPA–MNP [$(CH_3)_3C(CH_2OH)$–$(NO_2)(CH_3)_2C(CH_2OH)$] is almost flat, which is completely reasonably taking into account that the number of available groups to generate dynamical hydrogen bonds is equal. In addition, Fig. 7 shows that the packing variation for each system does not deviate noticeably from linear behaviour (Vegard's law) in spite of the large molecular volume differences. This result implies that the lattice deformation due to steric factors is not important. Also according to Kitaigorodsky[55] the steric factor (shape and size of molecules) can be analysed by a coefficient similarity ε_K, the so-called degree of molecular homeomorphism. Such a coefficient is calculated as $\varepsilon_K = 1 - \Gamma/\Delta$, where Γ is the non-overlapping part and Δ is the overlapping part when the molecules are superimposed so as to maximise the overlapping parts. Kitaigorodsky proposed a limiting value of 0.85 to achieve complete miscibility. As can be seen in Table 2, the ε_K values range between 0.826 and 0.976 and, therefore the limiting value previously mentioned does not account for the miscibility of orientationally disordered phases. This result is completely reasonable if we consider that in the substitution process, which takes place in the formation of disordered mixed crystals, the symmetry simulation is already present owing to the overall tumbling motion of the molecules in such a disordered phase, *i.e.*, the shape of the molecule is not well defined and the steric conditions will be totally controlled by the molecular size, a parameter which is included in the packing coefficient calculation.

As a conclusion of these results when continuous disordered mixed crystals from $x=0$ to 1 are formed (*i.e.*, the existence of isomorphism), the intermolecular interactions control the structure of the orientationally disordered molecular alloys. Such a conclusion was already announced for ODICs in the case of molecular alloys between non-isomorphous plastic phases.[19] To go further into the research in two-component systems of this type of materials, an approach connecting this structural parameter with the thermodynamic properties has been performed and is presented in the following paper.

Acknowledgements

This work has been performed within the framework of the Réseau Européen sur les Aliages Moléculaires (REALM). We acknowledge the financial support of the DGICYT Grant PB95-0032.

References

1 J. Timmermans, *J. Phys. Chem. Solids*, 1961, **18**, 1.
2 L. A. K. Staveley, *Annu. Rev. Phys. Chem.*, 1962, **13**, 1.
3 N. G. Parsonage and L. A. K. Staveley, *Disorder in Crystals*, Clarendon, Oxford, 1978.
4 W. J. Dunning, *J. Phys. Chem. Solids*, 1961, **18**, 21.
5 M. Barrio, D. O. López, J. Ll. Tamarit, P. Negrier and Y. Haget, *J. Mater. Chem.*, 1995, **5**, 431.
6 J. Reuter, D. Busing, J. Ll. Tamarit and A. Würflinger, *J. Mater. Chem.*, 1997, **7**, 41.
7 A. Würflinger, *Int. Rev. Phys. Chem.*, 1993, **12**, 89.
8 T. Hasebe, G. Soda and H. Chihara, *Bull. Chem. Soc. Jpn.*, 1981, **54**, 2583.
9 D. W. Akness and L. L. Kimtys, *Acta Chem. Scand. Ser. A.*, 1980, **34**, 589.
10 J. Ll. Tamarit, M. A. Pérez-Jubindo and M. R. de la Fuente, *J. Phys. Condens. Matter.*, 1997, **9**, 5469.
11 J. Ll. Tamarit and A. Würflinger, *XXIV Journées d'Étude des Equilibres entre Phases, Nancy* (*France*) 2–3 April, 1998, p. 271.
12 U. T. Höchli, K. Knorr and A. Loidl, *Adv. Phys.*, 1990, **39**, 405.
13 H. Suga and S. Seki, *J. Non. Cryst. Solids*, 1974, **16**, 17.
14 M. Foulon, J. P. Amoreux, J. L. Sauvajol, J. Lefebvre and M. Descamps, *J. Phys. C: Solid State Phys.*, 1983, **16**, L265.
15 D. Mondieig, P. Espeau, L. Robles, Y. Haget, H. A. J. Oonk and M. A. Cuevas-Diarte, *J. Chem. Soc., Faraday Trans.*, 1997, **93**, 3343.
16 H. A. J. Oonk, D. Mondieig, Y. Haget and M. A. Cuevas-Diarte, *J. Chem. Phys.*, 1997, **108**, 715.
17 W. J. M.van der Kemp, J. G. Bolk, P. R. van der Linde, H. A. J. Oonk, A. Schuijff and M. L. Verdonk, *Calphad*, 1994, **18**, 255.
18 M. Barrio, D. O. López, J. Ll. Tamarit, P. Negrier and Y. Haget, *J. Solid State Chem.*, 1996, **124**, 29.
19 J. Salud, D. O. López, M. Barrio, J. Ll. Tamarit, P. Negrier and Y. Haget, *J. Solid State Chem.*, 1997, **133**, 536.
20 R. Courchinoux, N. B. Chanh, Y. Haget, T. Calvet, E. Estop and M. A. Cuevas-Diarte, *J. Chim. Phys.*, 1989, **86**, 561.
21 J. Ballon, V. Comparat and J. Pouxe, *Nucl. Instrum. Methods*, 1983, **217**, 213.
22 P. Deniard, M. Evrani, J. M. Barbe and R. Brec, *Mater. Sci. Forum*, 1991, **79–82**, 363.
23 M. Evani, P. Deniard, A. Jouanneaux and R. Brec, *J. Appl. Crystallogr.*, 1993, **26**, 563.
24 M. Jenau, J. Reuter, J. Ll. Tamarit and A. Würflinger, *J. Chem. Soc., Faraday Trans.*, 1996, **92**, 1899.
25 T. Hasebe and H. Chihara, *Bull. Chem. Soc. Jpn.*, 1986, **59**, 1141.
26 J. Mayer, I. Natkaniea, J. Sciesinski and S. Urban, *Acta Phys. Pol. A*, 1977, **52**, 655.
27 T. Hasebe, N. Nakamura and H. Chihara, *Bull. Chem. Soc. Jpn.*, 1984, **57**, 179.
28 D. Büsing, M. Jenau, J. Reuter, A. Würflinger and J. Ll. Tamarit, *Z. Naturforsch., Teil A*, 1995, **50**, 502.
29 J. Ll. Tamarit, N. B. Chanh, P. Negrier, D. O. López, M. Barrio and Y. Haget, *Powder Diffract.*, 1994, **9**, 1.
30 E. Lipczynska-Kochany and T. Urbanski, *Can. J. Chem.*, 1977, **55**, 2504.
31 T. Urbanski, E. Lipczynska-Kochany and W. Waclawec, *Bull. Acad. Pol. Sci.*, 1977, **25**, 185.

32 D. O. López, M. Barrio, J. Ll. Tamarit, P. Negrier and Y. Haget, *Mol. Cryst. Liq. Cryst.*, 1995, **268**, 129.
33 J. Salud, M. Barrio, D. O. López, J. Ll. Tamarit and X. Alcobé, *J. Appl. Crystallogr.*, 1998, **31**, 748.
34 K. Suenaga, R. Kanae, T. Matsuo and H. Suga, *IUPAC Conference*, Como, Italy, 1990.
35 D. Chandra, C. S. Day and Ch. S. Barret, *Powder Diffract.*, 1993, **8**, 109.
36 M. Barrio, J. Font, D. O. López, J. Muntasell, J. Ll. Tamarit, P. Negrier and Y. Haget, *J. Phys. Chem. Solids*, 1994, **55**, 1295.
37 D. Eilerman, R. Lippman and R. Rudman, *Acta Crystallogr., Sect. B*, 1983, **39**, 263.
38 M. Barrio, J. Font, D. O. López, J. Muntasell, J. Ll. Tamarit and Y. Haget, *J. Appl. Crystallogr.*, 1994, **27**, 527.
39 M. Barrio, J. Font, D. O. López, J. Muntasell, J. Ll. Tamarit, P. Negrier and Y. Haget, *J. Phys. Chem. Solids*, 1993, **54**, 171.
40 G. B. Carpenter, *Acta Crystallogr., Sect. B*, 1969, **25**, 163.
41 H. G. Kreul, R. Waldinger and A. Würflinger, *Z. Naturforsch., Teil A*, 1992, **47**, 1127; H. G. Kreul, Doctoral Thesis, University of Bochum, 1991.
42 K. Adachi, H. Suga and S. Seki, *Bull. Chem. Soc. Jpn.*, 1968, **41**, 1073.
43 M. Foulon, J. P. Amoreux, J. L. Sauvajol, J. P. Cavrot and M. Müller, *J. Phys. C: Solid State Phys.*, 1984, **17**, 4213.
44 M. Foulon, J. Lefebvre, J. P. Amoreux, M. Müller and D. Magnier, *J. Phys. Fr.*, 1985, **46**, 919.
45 C. A. Angell and W. Sichina, *Ann. New York Acad. Sci.*, 1976, **279**, 53.
46 C. A. Angell, *J. Phys. Chem.*, 1988, **49**, 863.
47 R. Strauss, S. Braun, S. Dou, H. Fuess and A. Weiss, *Z.Naturforsch., Teil A*, 1996, **51**, 871.
48 R. Zannetti, *Acta Crystallogr.*, 1961, **14**, 203.
49 J. Ll. Tamarit, M. Barrio, D. O. López and Y. Haget, *J. Appl. Crystallogr.*, 1997, **30**, 118.
50 J. Salud, Doctoral Thesis, Polytechnic University of Catalonia, in preparation.
51 S. Urban, Z. Tomkowicz, J. Mayer and T. Waluga, *Acta Phys. Pol. A*, 1976, **49**, 741.
52 M. Barrio, J. Font, D. O. López, J. Muntasell and J. Ll. Tamarit, *J. Chim. Phys.*, 1991,**87**, 1835.
53 J. F. Willart, M. Descamps and N. Benzakour, *J. Chem. Phys.*, 1996, **104**, 2508.
54 M. Descamps, J. F. Willart, G. Odou and K. Eichhorn, *J. Phys.*, 1981, C6, **42**, 63.
55 A. I. Kitaigorodsky, *Mixed Crystals*, Springer-Verlag, Berlin, 1984.
56 A. I. Kitaigorodsky, *Organic Chemical Crystallography*, Consultants Bureau, New York, 1961.
57 L. Pauling, *The Nature of the Chemical Bond*, Cornell University Press, Ithaca, 1968.
58 A. Bondi, *Physical Properties of Molecular Crystals, Liquids and Glasses*, Wiley, New York, 1969.

Paper 8/08258H